Preparation and Characterization of Carbon Nanofiber Reinforced Thermoplastic Polyurethane Nanocomposites

A. K. Barick,[1] D. K. Tripathy[1,2]

[1]*Rubber Technology Centre, Indian Institute of Technology, Kharagpur 721302, West Medinipur, West Bengal, India*
[2]*Vice Chancellor, Veer Surendra Sai University of Technology, Burla 768018, Sambalpur, Odisha, India*

Received 20 August 2010; accepted 11 June 2011
DOI 10.1002/app.35066
Published online 10 October 2011 in Wiley Online Library (wileyonlinelibrary.com).

ABSTRACT: The effect of CNFs on hard and soft segments of TPU matrix was evaluated using Fourier transform infrared (FTIR) spectroscope. The dispersion and distribution of the CNFs in the TPU matrix were investigated through wide angle X-ray diffraction (WAXD), field emission scanning electron microscope (FESEM), high resolution transmission electron microscope (HRTEM), polarizing optical microscope (POM), and atomic force microscope (AFM). The thermogravimetric analysis (TGA) showed that the inclusion of CNF improved the thermal stability of virgin TPU. The glass transition temperature (T_g), crystallization, and melting behaviors of the TPU matrix in the presence of dispersed CNF were observed by differential scanning calorimetry (DSC). The dynamic viscoelastic behavior of the nanocomposites was studied by dynamical mechanical thermal analysis (DMTA) and substantial improvement in storage modulus (E') was achieved with the addition of CNF to TPU matrix. The rheological behavior of TPU nanocomposites were tested by rubber processing analyzer (RPA) in dynamic frequency sweep and the storage modulus (G') of the nanocomposites was enhanced with increase in CNF loading. The dielectric properties of the nanocomposites exhibited significant improvement with incorporation of CNF. The TPU matrix exhibits remarkable improvement of mechanical properties with addition of CNF. © 2011 Wiley Periodicals, Inc. J Appl Polym Sci 124: 765–780, 2012

Key words: nanocomposites; nanofiber; mechanical properties; thermal properties; rheology

INTRODUCTION

Nanostructured materials gained remarkable importance in the present decade on account of their broad range of potential applications in many strong hold areas. A large interest is devoted to carbon based nanomaterials that exhibit exceptional electrical and mechanical properties and can therefore be used for the development of a new generation composite materials. Since carbon nanofiber (CNF) has extraordinary mechanical properties, it can be judiciously used as reinforcement in polymers and other matrices to form so-called "nanocomposite materials".[1] Polymer nanocomposites are a novel class of composite materials where one part of the constituents has dimensions in the range of 1–100 nm.

The investigation of especially CNF has opened a totally new window for the development of polymer matrix composites with excellent material properties and applications. The extent of improvement of properties depend on several interlinked parameters including the size of the particles, their aspect ratio, their degree of dispersion and orientation in the matrix and the degree of adhesion with the polymer chains. To develop polymer nanocomposite materials with excellent mechanical properties, strong chemical bonding between the reinforcement and the matrix is a necessary, but not the sufficient enough condition.

The literature survey reveals that a very few research works have been reported regarding polyurethane matrix. Gunes et al.[2] have evaluated the effects of thermal expansion on shape-memory performance of polyurethanes and their nanocomposites with CNF. It was observed that the presence of CNF drastically reduced the soft segment crystallinity leading to a remarkable reduction in the shape recovery ratio and the recovered strain. Gunes et al.[3] have also reported the effectiveness of carbonaceous, electrically conductive fillers in shape memory actuation of polyurethane composites prepared by resistive heating. The relationships between soft segment crystallinity and the electrical percolation behavior of SMPU composites filled with CNF and oxidized CNF (ox-CNF) were also presented. Jimenez and Jana[4] have studied composites of ox-CNFs thermoplastic polyurethane (TPU) prepared in a chaotic mixer and have compared their electrical and

Correspondence to: D. K. Tripathy (dkt@rtc.iitkgp.ernet.in or vcvssut@gmail.com).

Contract grant sponsor: Council of Scientific and Industrial Research (CSIR), New Delhi, India; contract grant number: 22(0410)/06/EMR-II dated 13/09/2006.

mechanical properties with those prepared using untreated CNFs. Consequently, dispersion of ox-CNFs improved in the polymers and the resultant composites showed improved thermal-oxidative stability, higher storage modulus, and higher T_g. The electrical conductivity, however, decreased with improved nanofiber dispersion. Jimenez and Jana[5] have also studied composites of CNFs, ox-CNFs, and shape-memory TPU prepared in a chaotic mixer and have evaluated shape-memory properties. The shape-memory action was triggered by both conductive and resistive heating. It was found that soft segment crystallinity and mechanical reinforcement by CNFs produced competing effects on shape memory properties. Powers et al.[6] have employed solid-state proton nuclear magnetic resonance (NMR) to investigate the structure and dynamics of a thermoplastic polyurethane elastomer (TPE) filled with CNFs for shape memory applications. Furthermore, in our previous work the TPU/CNF nanocomposite was extensively studied with reference to morphology, thermal, electrical, and mechanical properties.[7]

In this article, we report the preparation and characterization of TPU nanocomposites with various weight percent loadings of CNFs formed using internal batch mixing followed by compression molding. Different sophisticated technical methods were adopted to find out the effect of type and concentration of CNF on thermal, dynamic mechanical, rheological, electrical, and mechanical properties. The main objective is to significantly improve the material properties with low nanofiber loadings. The probable applications of the nanocomposites are in biomedical, packaging, electrical, and etc.

EXPERIMENTAL

Materials

Commercial biomedical clear grade aliphatic polyether-based TPU (Tecoflex® TPU EG 80A injection grade) with around 35% of hard segments used as the matrix for this work was procured from Lubrizol Advanced Materials, Inc., Thermedics® Polymer Products, USA. Tecoflex® TPU EG 80A has Shore A hardness of 72, density of 1.04 g/cm^3 and it was synthesized from 4,4′-Methylene-bis(cyclohexyl isocyanate) (hydrogenated MDI, H12MDI) hard segment, polytetramethylene glycol (PTMG) soft segment (molecular weight = 1000 g/mol), and chain extender 1,4 butane diol (BD).

Vapor-grown CNF (Pyrograf-III™ CNF, PR-24 nanofiber type and LHT low heat treated graphitized fiber grade) was procured from Pyrograf® Products an affiliate Applied Sciences, USA. PR-24-LHT-XT-LD low density hydroxyl (–OH) modified CNFs having average fiber diameter of 100 nm, surface area of 35–45 m^2/g, dispersive surface energy of 145–165 mJ/m^2, length of 3×10^4–10^5 nm, iron content of = 14×10^3 parts per million (PPM), moisture content of = 5 wt %, and polycyclic aromatic hydrocarbons (PAH) content of = 1 mg PAH/g of fibers has been used for the research work. The nitric acid (HNO_3), sulfuric acid (H_2SO_4), and dichloromethane (CH_2Cl_2) solvent used were procured from Merck Specialities Private Limited, India.

Purification and functionalization of CNF

The purification and functionalization processes are very much necessary to separate the unwanted waste products like amorphous carbon and activate functional groups for the better utilization of vapor-grown CNF (VGCNF), which provide opening of the highly tangled nests like three dimensional network structures of nanofibers without shortening its length. Both purification and functionalization method of CNF as reported by Lozano et al. was adopted for carrying out the same.[8] Purification was conducted by refluxing CNFs in dichloromethane (CH_2Cl_2) for 5 days at 35°C followed by thorough washings using deionized water and refluxing further for a period of 24 h at 90°C. The CNFs were rinsed again with deionized water and vacuum filtered using Whatman quantitative filter paper for 24 h and dried in circulating hot air oven at 120°C for 48 h. Functionalization was conducted by refluxing CNFs in the mixtures of HNO_3 (65% solution or concentrated), H_2SO_4 (65% solution) acids to activate functional groups present on the nanofibers.

Preparation of TPU nanocomposites

TPU/CNF nanocomposites of different formulations were prepared using melt intercalation technique by mixing the VGCNFs with the TPU matrix in a Thermo Scientific Haake PolyLab OS Rheomix (Thermo Electron Corporation, USA) internal batch mixer at 185°C with a rotor speed of 100 rpm and mixing time of 8 min. Different compositions by weight percent (wt %) were prepared by taking 1, 4, 7, 10, and 15 wt % of nanofibers in 100 phr (parts per hundred) of TPU matrix. The pristine TPU pellets were also melt compounded to minimize the interference of processing parameters that required for the comparison of the properties with that of nanocomposites. TPU pellets and VGCFs were dried at 80 and 120°C in a preheated vacuum oven for 6 and 24 h, respectively before processing to remove the moisture content if any in the supplied materials. The compounds were passed once through a cold two-roll mill (Farrel Bridge Limited, England) immediately after batch mixing to achieve thick sheets. Sheet specimens of thickness about 2 mm for all the compositions were prepared using compression molding machine (Moore Press, GE Moore and

Son, UK) at 185 °C with a pressure of 5 MPa for 3 min. The sheets were cooled to room temperature under adequate pressure with controlled supply of circulating water. The specimens for mechanical testing were punched from the compression molded sheets. The virgin sample is represented as "TPU" and TPU nanocomposite samples are named as "TPUXL"; where "X" stands for wt % of CNF in TPU matrix and "L" stands for PR-24-LHT-XT-LD Pyrograf® VGCNF.

Measurements and characterization

An infrared (IR) spectrum of CNF is recorded using fourier transform infrared spectroscopy (FTIR) spectrophotometer (spectrum RX-I, PerkinElmer Life and Analytical Sciences, USA) to evaluate the purification and functionalization processes of CNF. FTIR spectrometer (Nexus-870, Thermo Nicolet Corporation, USA) equipped with an ATR (attenuated total reflectance) probe was used to evaluate the interfacial interactions between CNF and TPU matrix. The band intensities are assigned as strong (s), medium (m), weak (w), shoulder (sh), variable (v), sharp (shp), and broad (br). The types of vibrations are designated as stretch (str), bending (bend), and out-of-plane bending (op). Wide angle X-ray diffraction (WAXD) analysis was performed with a high-resolution X-ray diffractometer (X'Pert PRO, Philips PANalytical B.V., Netherlands) using Cu-Kα ($\lambda = 1.54$ Å) radiation source. The field emission scanning electron microscope (FESEM) (Supra 40, Carl Zeiss SMT AG, Germany) was employed to evaluate the nanostructure morphology of the TPU/CNF nanocomposites. The cryofractured surface of samples for FESEM were gold (Au) coated by means of auto sputter coater of gold–palladium (Pd) target (SC7620, Polaron Brand, Carbon Accessory, Quorum Technologies, UK). The distribution of nanofiber within the TPU matrix and interfacial region of nanofiber and matrix was studied using a high resolution transmission electron microscope (HRTEM) (JEM 2100, JEOL Limited, Japan) attached with charge couple device (CCD) camera (Gatan, USA). The samples for HRTEM analysis were prepared using an ultramicrotome (Ultracut UCT, Leica Microsystems GmbH, Austria). Atomic force microscope (AFM) topographic images were obtained using a near-field scanning optical microscope (NSOM)/scanning probe microscope (SPM) (NSOM/SPM-100 Confocal™ (MultiView 1000™), Nanonics Imaging Ltd., Israel) attached with CCD color video camera (KY-F55B, Victor Company of Japan Limited (JVC), Japan). Polarizing optical microscope (POM) surface morphology of samples were studied using compound polarized light microscope (DMLM, Leica Microsystems GmbH, Germany) attached with CCD color camera (KY-F550E, JVC). Thermal stability and composition of TPU and TPU/CNF nanocomposites were measured by thermogravimetric analysis (TGA) (Q50, V6.1 series, TA Instruments, USA). The T_g, melting point and crystallization temperature of nanocomposite samples were evaluated by means of differential scanning calorimetry (DSC) (Q100, V8.1 series, TA Instruments). Dynamic mechanical properties of nanocomposites were measured by dynamical mechanical thermal analysis (DMTA) (2980, V1.7B series, TA Instruments). The viscoelastic properties of the samples were studied using a rubber processing analyzer (RPA) (RPA 2000, Alpha Technologies, USA). The alternating current (AC) conductivity (σ), dielectric constant or permittivity (ε′), dielectric loss (ε″) and dissipation factor (DF) of neat TPU and TPU/CNF nanocomposites were measured with a LCR meter (7600 precision LCR Meter, model B, QuadTech, USA). The tensile properties of the samples were determined according to American society for testing and materials (ASTM) standard ASTM D-412-98a(2002) test procedure using an universal testing machine (UTM) (4468, Instron Corporation, USA). The tear tests of the samples were carried out by an Instron UTM according to the ASTM D624-00(2007) specification. The hardness of the samples were measured by Shore A durometer hardness tester (SHR-A-SUPER-Y_2K, TRSE Testing Machines, Blue steel Engineers, India) as per ASTM D2240-05(2010) standard.

RESULTS AND DISCUSSION

Spectroscopic characterization

Fourier transform infrared spectroscopy

The chemical structures of the nanocomposites of CNF and TPU as well as pristine CNF and TPU are analyzed by an FTIR spectrometer. FTIR (KBr, cm^{-1}): 2853 (s), 2921 (s), and 2955 (w) (str, sp^2 C—H (>CH_2) and sp^3 C—H (—CH_3)); 2360 (s, shp, str, CO_2); 1460 (bend, v, >CH_2 or —CH_3); 868 (op, w, isolated aromatic C—H); 1590 (s) and 1406 (sh) (str, aromatic carbon skeleton (—C—C—)); 1262, 1119, 1092, and 1019 (br, str, C—O or C—O—C of ester, ether, and phenol or carboxyl groups); 3441 (s, br, str, —OH of carboxylic and phenolic groups or adsorbed water); 1734 (s, str, >C=O of carboxyl, lactone or ketone groups); and 1654 (s, str, >C=O of quinine or conjugated ketone).

The TPU and TPU/CNF composites show the following characteristic IR absorption frequencies. ATR-FTIR (cm^{-1}): 3455 (w, str, free —NH—) and 3320 (m, str, hydrogen bonded —NH—); 1714 (s, str, free >C=O) and 1697 (s, str, hydrogen bonded >C=O); and 1666 (s, str, —HN—C=O). The absorption peaks concerned with the amine (—NH) and carbonyl (>C=O) groups are the main matter of consideration to evaluate the extensive intermolecular hydrogen bonding tendency of the TPU matrix.

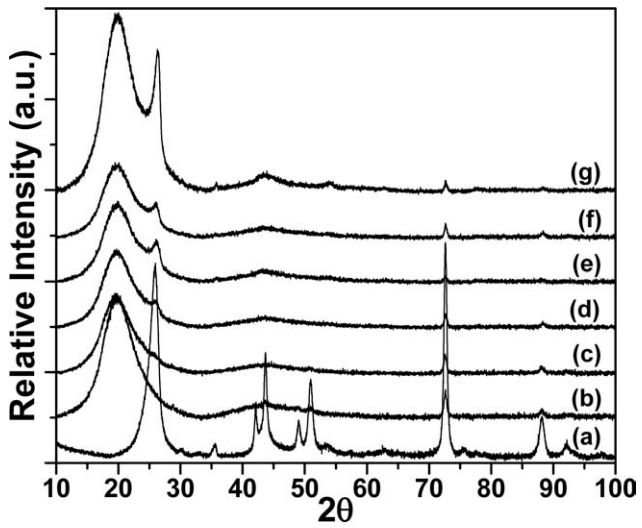

Figure 1 WAXD patterns of (a) neat CNF, (b) pure TPU, and TPU/CNF nanocomposites with (c) 1 wt %, (d) 4 wt %, (e) 7 wt %, (f) 10 wt %, and (g) 15 wt % CNF loading.

Hydrogen bonding involves the —NH— group present in urethane linkage as donor part, and the urethane carbonyl (>C=O) and the ether oxygen (—O—) in polyether urethane as the acceptor site. The peak corresponds to the free —NH group is diminished and the peak assigned for hydrogen bonded —NH group in case of neat TPU and TPU/CNF nanocomposites is present, which indicates that the majority of —NH groups in urethane linkages (—HN—COO—) participated in hydrogen bonding with the >C=O group of the hard segments or with the ether linkages (—O—) of the soft segments or with the hydrogen of the hydroxyl (—OH) group present in the CNFs surface. The presence of both free and bonded types of >C=O groups in the TPU matrix concludes that the microphase separation occurred between the soft and hard segments of the TPU matrix. The IR peak at around 3441 cm^{-1} disappeared in the TPU/CNF nanocomposites indicating that a good interfacial interaction existed between the TPU matrix and CNF surface.

Morphological characterization

Wide angle X-ray diffraction

Figure 1 displays the WAXD patterns of neat TPU, CNF, and TPU/CNF nanocomposites containing various dose of CNF loading to observe the effect of CNF content. The WAXD plot of neat TPU clearly shows a strong broad diffraction peak at $2\theta = 19.75^\circ$ ($d_{110} = 4.495$ Å) corresponding to the mixture of both short range ordered regular structure of hard phase and disordered irregular structure of amorphous phase of TPU matrix.[9] Neither the peak position shifts with increase in CNF loading nor the peak gets broaden or reduced in intensity indicating that the amorphous structures of both the soft and hard segments are not disturbed through the incorporation of nanofibers. The absence of any sharp peak concludes that the TPU matrix has no crystalline structure. Almost all the peaks appear at the same location in the TPU/CNF nanocomposites implying the microstructure of the TPU is not sufficiently affected by introduction of CNF.

The WAXD pattern for CNF demonstrates a prominent sharp (0 0 2) Bragg diffraction peak at $2\theta = 25.90^\circ$ ($d_{002} = 3.44$ Å) corresponds to the ordered arrangement of different crystal surface of the concentric cylinders of crystal graphitic carbons.[10] This peak position is diminished in 1 wt% filled nanocomposites due to the low loading of CNFs and the intensity of the same diffraction peak is gradually increased with increase in CNF content because the fraction of CNF present in nanocomposites is of maximum 15 wt %. The diffraction peaks above $2\theta = 30^\circ$ are significantly affected by the nanocomposites preparation. Either the diffraction peaks became broad or the peak intensity is reduced compared with the original peaks in pristine CNF probably due to the breakdown of the crystal structure through the efficient mixing method.

Field emission scanning electron microscopy

The FESEM image of pure nanofibers is shown in Figure 2. It shows that all pristine nanofibers have high aspect ratio as large as 100 or higher. The diameters of the nanofibers vary from several tens of nanometers to a few hundred nanometers. The neat CNFs are shown as interwoven bundles and highly aggregate structures or clusters of several tens of microns in diameter. Some catalyst impurity and amorphous carbons also may be present on the CNF surface. The cryofractured surfaces of the compression molded TPU/CNF nanocomposite samples examined in FESEM are shown in Figure 3 to assess the degree of dispersion

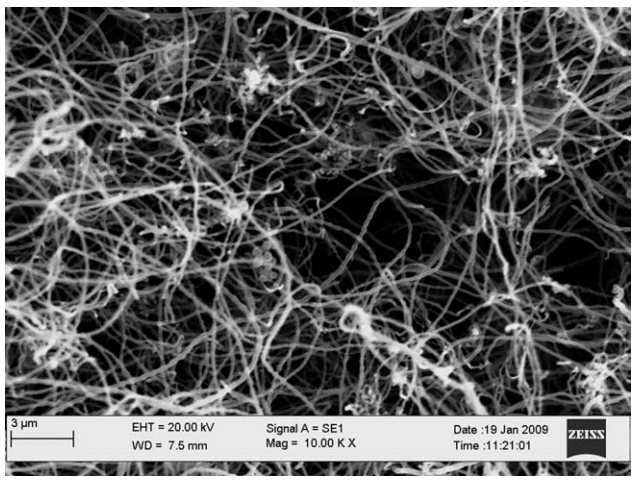

Figure 2 FESEM microphotograph of the neat VGCNF.

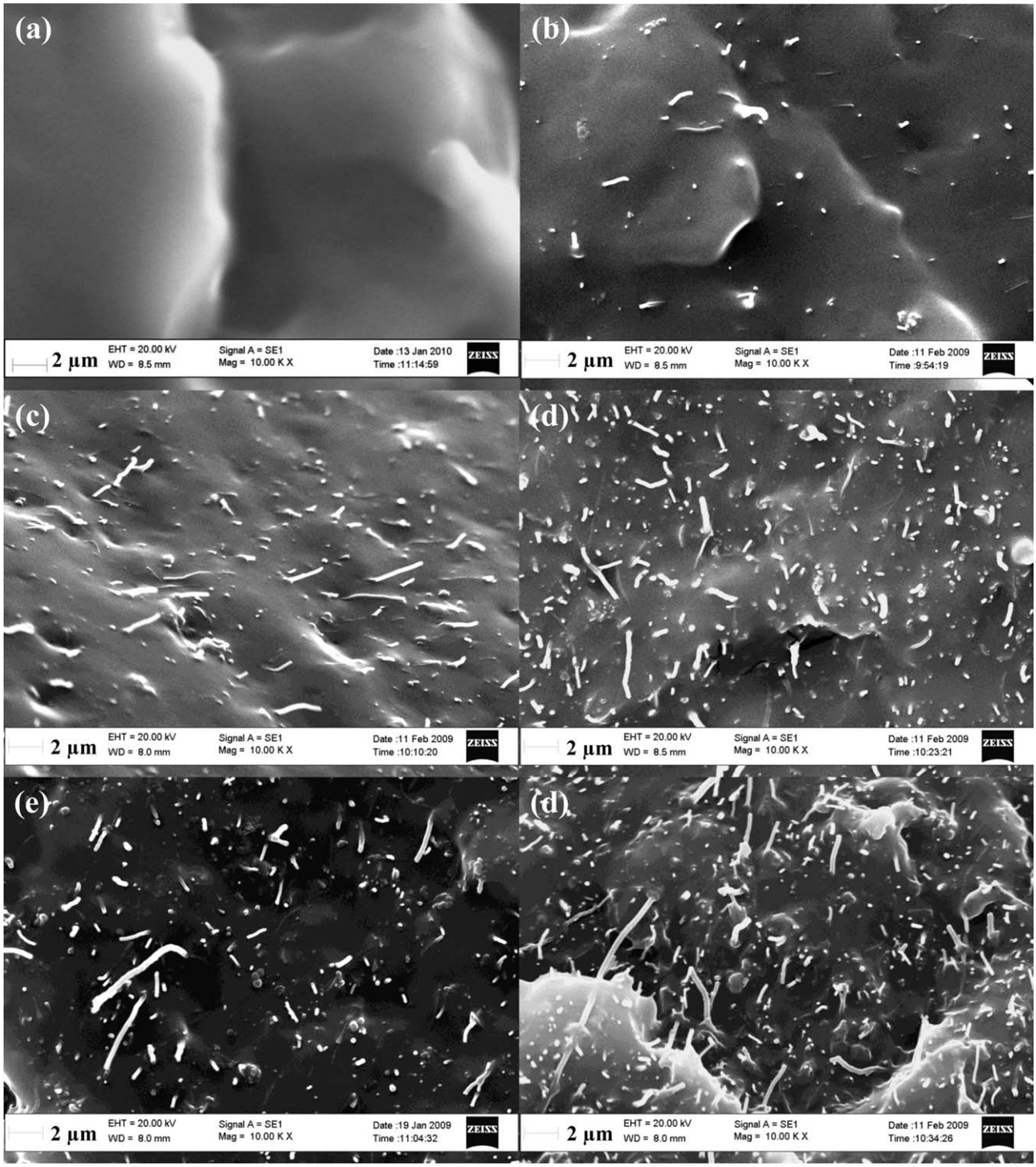

Figure 3 FESEM microphotographs of (a) neat TPU and TPU/CNF nanocomposites with (b) 1 wt %, (c) 4 wt %, (d) 7 wt %, (e) 10 wt %, and (f) 15 wt % CNF loading.

and alignment of the nanofibers achieved during melt processing. It is clearly observed from microphotographs that the nanofibers are dispersed homogeneously and evenly into the TPU matrix without any signs of agglomerations, although occasional small aggregates are observed in the nanocomposites filled with 10 and 15 wt % CNFs. The agglomerates are separated into individual nanofibers that uniformly dispersed and distributed within the TPU matrix, which is due to the high shear force developed during the melt compounding process. However, at high nanofiber loading some randomly distributed small aggregates are present as well as interconnected nanofiber conductive network structure is developed within the TPU matrix. The voids, cavities and holes are not visible around almost all of the nanofibers, which may be

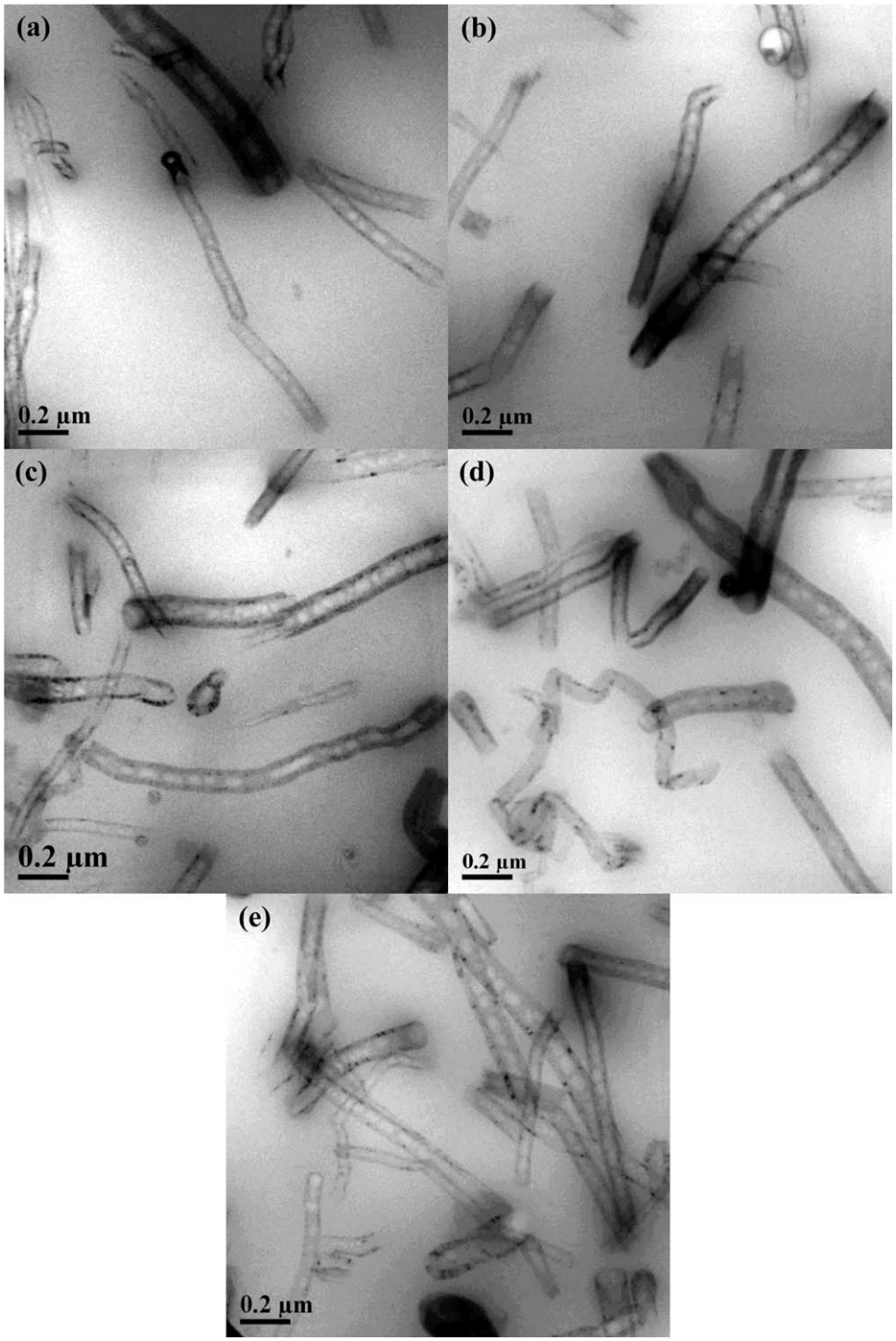

Figure 4 HRTEM microphotographs of TPU/CNF nanocomposites with (a) 1 wt %, (b) 4 wt %, (c) 7 wt %, (d) 10 wt %, and (e) 15 wt % CNF loading.

attributed to the better wetting and strong interphase bonding between nanofibers and TPU matrix.[5] The bulging white dots or lines on the FESEM microphotographs suggest that the embedded CNFs are encased by the folding or coiling within the TPU matrix. The majorities of the nanofibers observed in the cryofractured surface are well covered up by the thick layer of TPU on its base attached to the TPU matrix surface, which also indicates some degree of wetting and interphase adhesion among TPU matrix and CNF. The CNF are observed to be broken rather than just pulled out of the TPU matrix under breaking the specimens, which also indicates that the interfacial interaction of CNFs with TPU matrix is very strong enough. The nanofiber length distribution was affected by the shearing action during melt mixing

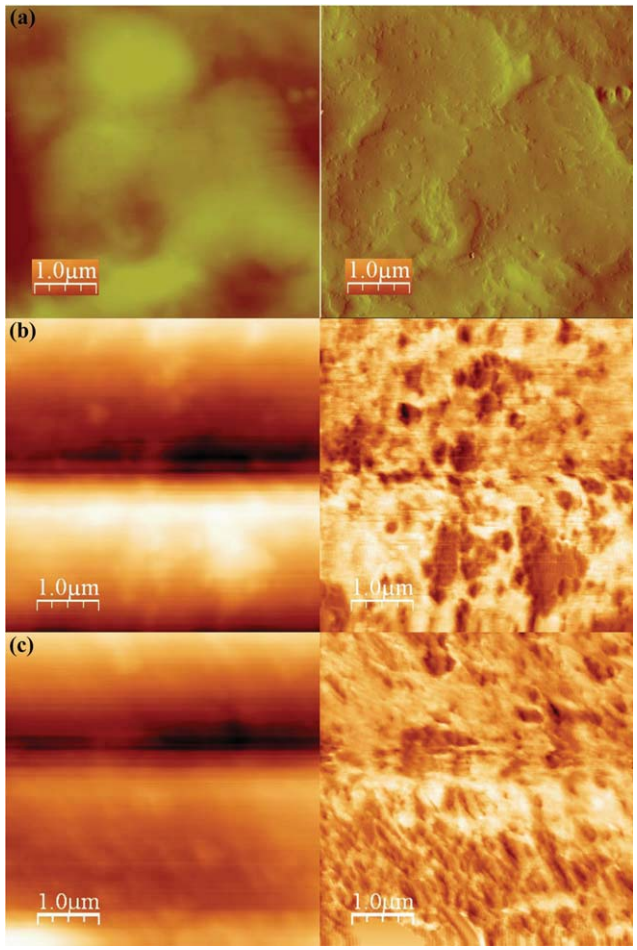

Figure 5 AFM images represent height images (left) and phase images (right) of (a) Pure TPU and TPU/CNF nanocomposites with (b) 4 wt % and (c) 10 wt % CNF loading. [Color figure can be viewed in the online issue, which is available at wileyonlinelibrary.com.]

process as a result the CNF aspect ratio is reduced significantly.

High resolution transmission electron microscopy

Figure 4 shows TEM micrographs of TPU/CNF nanocomposites of various wt% CNF loading. As noticed from the images for the nanocomposites loaded with 1–15 wt % CNFs, the nanofibers are well dispersed and distributed in the TPU matrix. Individual nanofibers are clearly observed throughout the samples with low wt % CNF concentration and dispersed well in the polymer matrix as well as small CNF aggregates at high nanofiber loading due to van der Waals force of attraction among them. CNFs may be effectively dispersed either covalent bond or ionic bond formation between CNF and TPU. It is observed that the aspect ratio of the nanofibers in the TPU/CNF nanocomposites are reduced as compared with the original length of the CNFs because of the high shearing action at the time of melt blending, which on the other way produced good nanofiber dispersion within the matrix.

Atomic force microscopy

AFM was applied to probe the morphology and dispersion of CNFs embedded in the TPU/CNF nanocomposites. Figure 5 shows simultaneously acquired topography (height image) as well as phase contrast images of the neat TPU and TPU/CNF nanocomposite samples. It is observed that the surface of the TPU nanocomposites became rougher than that of the neat TPU by the addition of CNFs. The microscopic examination across the length scales conferred that the CNFs are well distributed and dispersed over a considerable extent on the surface in all directions within the TPU matrix and even single CNFs are distinguishable from each other. The nanofibers are preferentially associated with the soft segment of the TPU matrix that developed sufficient wetting and interphase adhesion of the CNF with TPU. Also the association of the CNFs plays a good role in mechanical reinforcement with TPU matrix.

Polarizing optical microscopy

Figure 6 represents optical microphotographs of the surface of compression molded films of neat TPU and TPU nanocomposites containing 1–15 wt % CNF. It revealed that CNFs are uniformly dispersed within the TPU matrix. The variation in the length of observed CNF suggests that the breakage of nanofibers occurred during high shear mixing. The POM images clearly show the presence of aggregates/agglomerates of CNFs and it becomes more with increasing in higher wt % of CNF concentration. In case of neat TPU a spherulitic morphology is observed where globular hard segments are homogeneously distributed within the soft segment of TPU matrix. However, this type of morphology is totally disturbed by the presence of CNFs. This result reveals that good dispersion of VGCNF effectively influence the growth of spherulites and hinders crystal lattice formation in soft segments. Very high aspect ratio of CNF and strong bonding interactions between CNF and TPU lead to the interfacial attachment of CNFs to soft segments surface that impose substantial confinement and restriction to the movement of TPU long chains as a result the spherulitic morphology has disappeared significantly.

Thermal characterization

Thermogravimetric analysis

The data available from the TGA scan include: $T_{5wt\%}$, the temperature at which 5% degradation of sample occurs, is measured from the intersection of

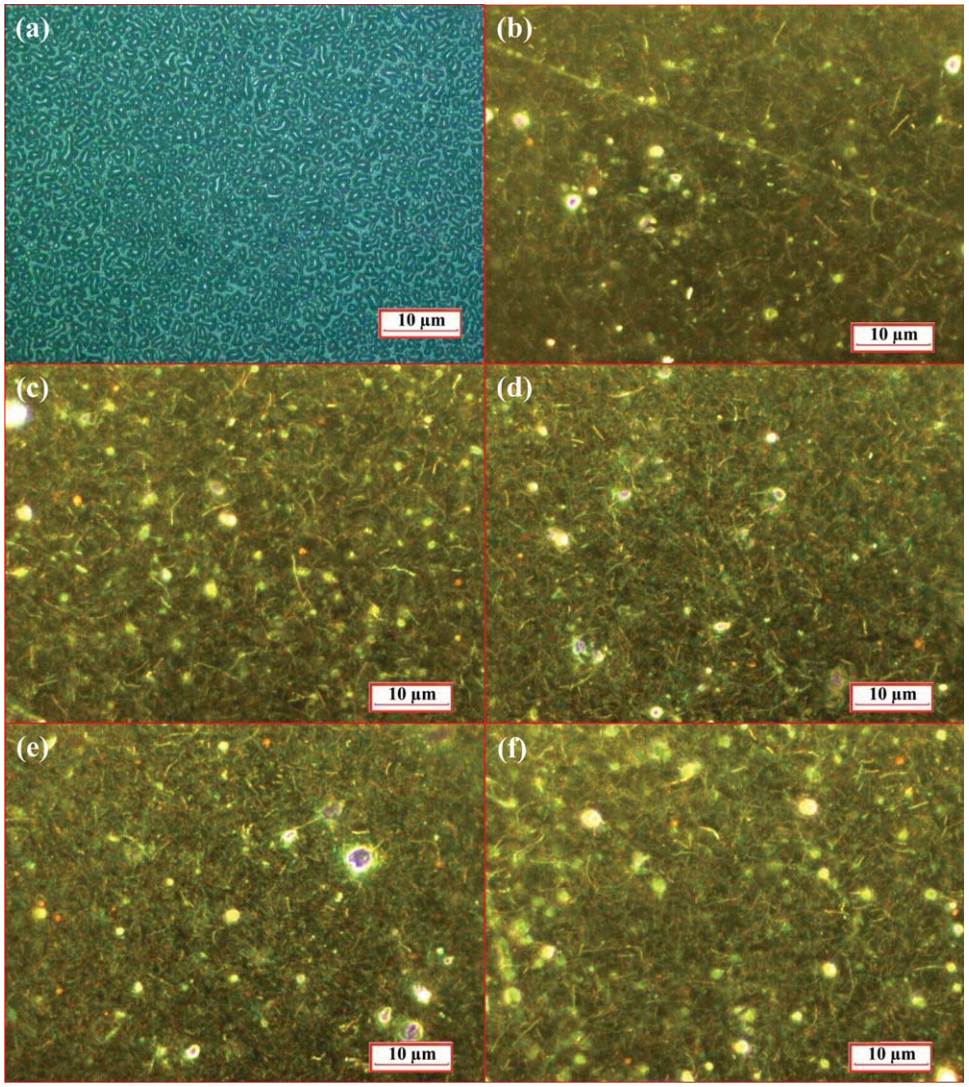

Figure 6 POM microphotographs of (a) neat TPU and TPU/CNF nanocomposites with (b) 1 wt %, (c) 4 wt %, (d) 7 wt %, (e) 10 wt %, and (f) 15 wt % CNF loading. [Color figure can be viewed in the online issue, which is available at wileyonlinelibrary.com.]

the tangent of the initial point and the inflection point that is considered as the onset temperature of thermal degradation; $T_{50wt\%}$, the temperature at which 50% degradation occurs, which is another calculation of thermal stability; $T_{95wt\%}$, the temperature at which 95% degradation occurs, which is calculated from the intersection of the tangent of the final point and is considered as the end temperature of degradation; $r_{500wt\%}$, the nonvolatile fraction at 500°C, denotes as residual char formation through decomposition process; and finally T^1_D and T^2_D, corresponds to the first and second derivative peak temperatures, respectively and was availed from the derivative thermogravimetric curves. These data are summarized in Table I. Table I indicate that the thermal stability of TPU matrix improved significantly

TABLE I
Data Summarized from TGA and DTG Thermograms of TPU and TPU/CNF Nanocomposites

Sample code	$T^1{}_D$ (°C)	$T^2{}_D$ (°C)	$T_{5wt\%}$ (°C)	$T_{50wt\%}$ (°C)	$T_{95wt\%}$ (°C)	$r_{500wt\%}$ (wt%)
TPU	321.371	408.65	297.31	386.73	425.58	0.80
TPU1L	335.04	419.89	298.11	409.25	439.49	1.116
TPU4L	347.46	421.30	301.28	412.46	443.03	1.867
TPU7L	343.53	428.70	320.31	421.51	504.65	6.257
TPU10L	359.47	426.48	313.66	420.52	520.45	9.120
TPU15L	346.07	432.42	322.22	425.73	515.54	12.75

TABLE II
Data Summarized from DSC Thermograms of TPU and TPU/CNF Nanocomposites

Sample code	$T_{g\ (soft)}$[a] (°C)	ΔC_p[b] (W/g)	$T_{g\ (soft)}$[c] (°C)	ΔC_p[d] (W/g)	$T_{m\ (soft)}$ (°C)	$\Delta H_{m\ (soft)}$ (J/g)	$X_{c,s}$ (%)	$T_{m(hard)}$ (°C)	$\Delta H_{m(hard)}$ (J/g)
TPU	−71	0.5200	−61	0.4922	22	14.42	8.39	240	7.231
TPU1L	−73	0.5730	−62	0.5058	22	2.775	1.631	240	6.766
TPU4L	−70	0.5562	−62	0.5347	21	2.112	1.280	232	7.038
TPU7L	−69	0.4960	−60	0.5409	23	1.252	0.783	248	9.632
TPU10L	−71	0.5157	−58	0.5325	22	4.235	2.738	239	5.655
TPU15L	−72	0.6524	−60	0.5285	23	1.913	1.310	251	0.907

[a] $T_{g(soft)}$ of soft segment of TPU obtained from second heating cycle.
[b] ΔC_p for the $T_{g\ (soft)}$ obtained from second heating cycle.
[c] $T_{g\ (soft)}$ of soft segment of TPU obtained from first cooling cycle.
[d] ΔC_p for the $T_{g(soft)}$ obtained from first cooling cycle.

after nanocomposite formation with the incorporation of 1–15 wt % CNF. The improvement in thermal stability of nanocomposites at all temperature ranges is due to the homogeneous dispersion of the highly distributed CNFs in the TPU matrix, which by nature has higher thermal stability.[11] The homogeneous dispersion of nanofibers in TPU matrix resulting in a highly network structure and CNFs also impose a restriction on the mobilization of TPU macromolecules that prevent the gaseous molecules to come in contact with outer atmosphere in degradation process. Furthermore, CNFs dispersed in a TPU matrix conduct heat uniformly and avoid heat concentration due to the high thermal conductivity of CNFs as a consequence the thermal stability of the TPU is improved by inclusion the CNFs.[12]

The first derivative TGA (DTG) of TPU and its nanocomposite samples are also important because they more clearly show the difference in thermal stability of all the components present in the TPU matrix. The pristine TPU shows a two step degradation process: the first degradation step is associated with the decomposition of soft segments and the second step is mainly due to the complete degradation of hard segments of the TPU chains. The first and second derivative peaks position shift to the higher temperature range, which indicates that the thermal stability of the both soft and hard domains in TPU matrix improved significantly after incorporation of nanofiber and also it increases with increase in CNF loadings. The substantial improvement in the thermal stability of TPU is very important for TPU nanocomposite from the industrial product application point of view.

Differential scanning calorimetry

The peak temperature of crystallization melting point ($T_{m(soft)}$ and $T_{m(hard)}$), the enthalpy associated with heat of crystallization melting point ($\Delta H_{m(soft)}$ and $\Delta H_{m(hard)}$), and degree of crystallinity ($X_{c,s}$ and $X_{c,h}$) of soft and hard segment of TPU matrix as well as T_g of the soft segment ($T_{g(soft)}$) and heat capacity (ΔC_p) associated with it are obtained from the DSC scans, which are listed in Table II. The degree of crystallinity of a polymer matrix is calculated from the melting heat of crystallization according to the following equation:

$$X_c(\%) = (\Delta H_m/(1-\varphi)\Delta H_0) \times 100 \quad (1)$$

where, φ is the weight fraction of CNF, ΔH_m is the enthalpy of crystallization melting of soft and hard segments and ΔH_0= 171.87 J/g is the melting heat of 100% crystalline TPU.[13]

It is observed from the Table II that the prominent soft segment T_g occurs at about –70°C for pristine TPU- and CNF-based TPU nanocomposites. The temperature of $T_{g(soft)}$ did not change with increase of CNF concentration as change in heat capacity associated with it is too low to detect the shifting of the $T_{g(soft)}$. The restriction effect imparted by the CNF on the soft domain is counteracted by the reduction of hard phase due to the disturbance of CNF as a result the T_g of soft phase has not changed remarkably.

The Table II indicates almost no changes in heat of fusion corresponding to melting of the hard domains at around 240°C. Therefore, it can be concluded that the presence of fillers has no impact on hard domains of TPU matrix. However, TPU/CNF nanocomposites show a remarkable reduction in heat of fusion corresponding to melting of soft segments at around 22°C, hence it is inferred that CNF addition to the TPU matrix decreased the overall crystallinity and possibly the crystal size. The CNFs were mixed in melt blending scheme for 8 min and high rates of atmospheric cooling with time scales of the order of few seconds may have provided smaller time as a result TPU chains did not get sufficient time to pack in highly regular manner and crystallize in highly viscous environment. The presence of CNF with highly distorted irregular shapes may prevent chain packing and ordering of soft domains of TPU matrix. The crystallinity of soft segment of CNF

based TPU nanocomposites after the second scan shows an significant decrease as compared to pristine TPU and it is concluded that the crystallinity of soft segment is attributed to the filler geometry, the number of filler particles per unit volume, and the nature of organic or polar functional groups on the surface of filler particles, each of these play crucial roles in determining the soft segment crystallinity.[14] The crystalline soft segment originated from PTMG diol as a result higher soft segment crystallinity is attributed to the higher degree of phase separation of the domains containing PTMG diol. The soft segment crystallinity of TPU is significantly reduced by the presence of CNF because acceleration of hydrogen bonding that arises between the ether groups of PTMG and —NH groups of urethane linkages, which promotes mixing of the soft and hard segments and consequently may cause a reduction of the soft segment crystallinity.[7]

The absence of any peak in the peak in the cooling cycle of the DSC thermogram indicates that there is no development of crystallinity in the cooling process. The ordered structure of the hard and soft segments of TPU is too small to rearrange in the cooling process. The T_g of the neat TPU and TPU/CNF nanocomposites obtained from the cooling process is observed at around –61°C, which is significantly lower than that of the T_g determined from the heating process because the T_g of the amorphous soft segments of the TPU matrix prominently depends on the way of the measurement methodology adopted to find out the same.[15]

Dynamic mechanical thermal analysis

Figure 7(a) shows the effect of nanofiber content on the value of in-phase response or storage modulus (E') of nanocomposites of TPU with CNF as a function of temperature. The significant enhancement of E' with nanofiber content indicates that addition of CNFs exhibit a strong reinforcing effect on TPU matrix throughout the scanned temperature range.[8] The interfacial interlocking arises due to the strong bonding among TPU matrix and modified CNFs, which enhances the volume fraction or restrict the effective matrix chain molecular mobility at the interphase region in nanocomposites that act as an additional reinforcement for mechanical stiffening of the TPU matrix.[16] The magnitude of elastic modulus reduces stepwise with rise in temperature because of the increase in amorphous soft segment chain mobility of TPU matrix. The magnitude of storage modulus corresponding to the T_g is reduced rapidly with rise of temperature, which is ascribed to an energy dissipation phenomenon involving cooperative segmental motions of the polymer backbone chains.[17] Especially, at higher temperature range, the rate of increase in E' with CNF loading is prominent as

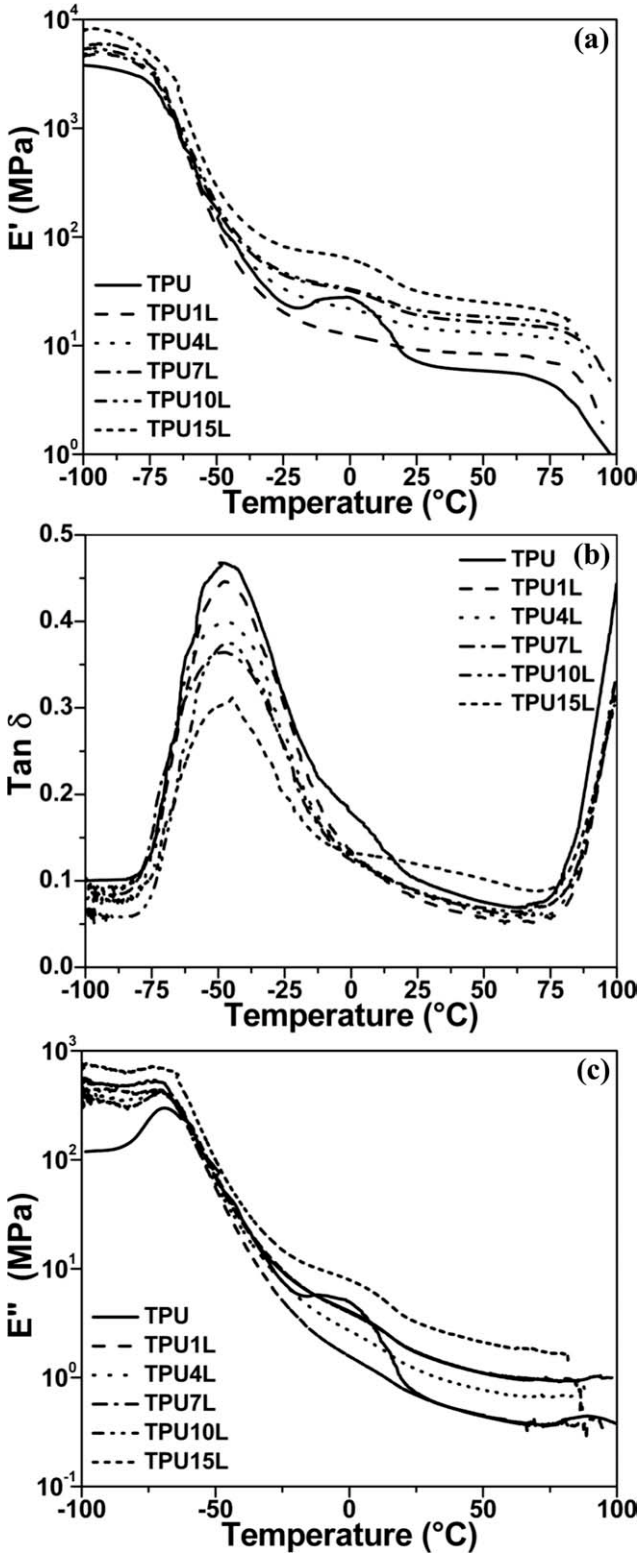

Figure 7 DMA thermograms represent the dependency of (a) E', (b) tan δ, and (c) E'' of neat TPU and TPU/CNF nanocomposites with 1, 4, 7, 10, and 15 wt % CNF loading on temperature at a given frequency and strain amplitude of 1 Hz and 10 μm, respectively.

compared with the lower temperature region because the presence of CNFs enable the TPU matrix to sustain stiffness. This exhibits a useful solid-state material property before approaching the softening temperature and as a consequence it enables the TPU matrix to sustain a high modulus value at high temperatures.[18] However, at around softening temperature the value of storage modulus tends to converge to that of the virgin TPU, which indicate that the modulus of the TPU/CNF nanocomposites are dominated by the matrix intrinsic modulus at high temperature range.[19]

The damping behavior or tangent of the ratio of the complex to real modulus (tan δ) of TPU/CNF nanocomposites is shown in Figure 7(b) as a function of CNF and temperature. A strong peak in tan δ curve is shown at around –48°C corresponds to the T_g of the soft segment present in the TPU matrix. The tan δ peak positions shift to the higher values with increase in wt % of CNF–OH loadings indicating higher soft segment T_g is attributed to the enhancement of hindered molecular chain mobility at the interphase of CNF and TPU matrix. The increase in tan δ peak values and reduction of areas under the tan δ curve with increase in CNF concentration is due to more homogeneous thermal energy distribution in TPU/CNF nanocomposites because thermal conductivity of CNF is very high than that of the pristine TPU counterpart.[17]

The out-of-phase response or dynamic loss modulus (E'') is a measure of the energy absorbed due to a relaxation and is useful in clarifying the mechanisms of internal motions. The loss modulus is found to increase along with the inclusion of nanofiber and with the increase of temperature as shown in Figure 7(c). This result indicates that the plastic response to the deformation is prominent in the presence of the nanofiber. The loss modulus of the TPU/CNF nanocomposites increased significantly with increasing CNF content at high temperature region. Furthermore, higher the values for loss modulus at higher temperatures (above T_g) suggest lower dampening characteristics of TPU nanocomposites containing higher CNF concentrations. The low temperature relaxation transition peak appearing at around –69°C in E'' curve is concerned with the dynamic complex multirelaxation process that mainly attributed to the molecular chain mobility of the crystalline segment of both soft and hard domains of the TPU matrix. The loss modulus peak position is not shifted significantly by the inclusion of CNF, which indicates that the addition of CNF has negligible effect on the dynamic relaxation behavior of the TPU matrix.[19]

Rheological characterization

Rubber processing analyzer

Dynamic frequency sweep tests were used to explore the crosslinked network formation and microstructure of the TPU/CNF nanocomposites in the linear viscoelastic region as well as to understand the processability of the nanocomposites. The storage modulus (G') and complex viscosity ($|\eta^*|$) obtained from the dynamic frequency scan measurements at 145°C for neat TPU and its nanocomposite samples containing various amounts of CNFs are shown in Figure 8(a,b). It is observed from the Figure 8(a) that the magnitude of G' significantly increases with increasing applied oscillatory frequency. The G' value increases monotonically with increase in CNF loading within the scanned frequency range. The high surface area and aspect ratio of the CNFs cause the formation of the percolation structure, which enhances the storage modulus of the nanocomposites. The degree of enhancement of storage modulus with frequency is more pronounced at lower frequency region than that of higher frequency range. At low frequencies, the G' increases monotonically with increasing CNF concentration while the slope of the line decreases. The storage modulus of homogeneously dispersed polymeric melt system exhibits a characteristic terminal flow behavior at low frequency regime due to the completely relaxed linear polymer chains. This phenomenon is in accordance to the theory of linear viscoelasticity i.e., the scaling law or power law relation of approximately $G' \propto \omega^2$ with slope of the plot equal to 2 for unfilled or uniformly dispersed polymer melts.[20] At low frequency region, the virgin TPU exhibits homopolymer-like typical terminal behavior with the scaling properties of $G' \sim \omega^x$. The power law index of $G'(\omega)$ for neat TPU is smaller than 2 ($x < 2$) because of the polydispersity of polymer chains. However, the terminal flow behavior of TPU/CNF nanocomposites significantly diminishes with the incorporation of CNF because of the microstructural changes developed in the TPU matrix. The slope of the plot in the terminal region significantly changed resulting in gradual minimization of dependence of G' on dynamic frequency. This may be attributed to the effective restrain applied on the large scale polymer relaxations by the presence of the nanofibers. The storage modulus plot of CNF filled TPU nanocomposites shift towards upward direction, which indicate that the CNFs form a pseudo-solid-like network in TPU matrix. The transition from the liquid-like to solid-like viscoelastic behavior at low frequency region is due to strong filler–filler and filler–polymer bonding interaction, which demonstrates that the dynamics of long-range polymer backbone chains is hindered prominently by the formation of the interconnected or network-like structures of CNFs.[21] The influence of nanofibers on the dynamic viscoelastic response of TPU/CNF nanocomposites is relatively weaker at high frequencies than the lower frequencies, reflects that

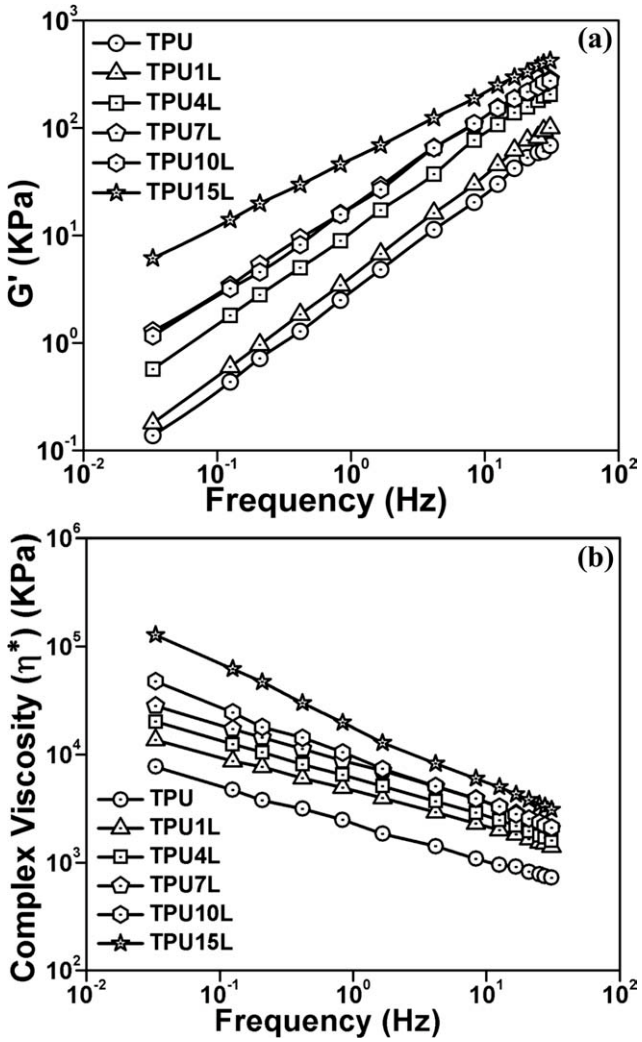

Figure 8 RPA rheographs depict the variation of (a) *G′* and (b) |η*| of neat TPU and TPU/CNF nanocomposites with 1, 4, 7, 10, and 15 wt % CNF loading with angular frequency at temperature and shear strain of 145°C and 0.98%, respectively.

the CNF has no substantial effect on the short range motion of the TPU chain entanglements.[22] The 15 wt % CNF-filled nanocomposites show good quantitative enhancement of *G′* value as compared to the nanocomposites filled up to 10 wt % CNF. The increase in modulus indicates threshold phenomenon especially for the storage modulus, which is termed as the rheological percolation threshold of modulus.[23] The rheological percolation threshold for TPU/CNF nanocomposites is about 10 wt % of CNF loading.

The variation of complex viscosity (|η*|) as a function of angular frequency and CNF concentration for neat TPU and TPU/CNF nanocomposites at 145°C is represented in Figure 8(b). The magnitude of viscosity decreases gradually with the increase in applied frequency that is termed as shear thinning characteristic or pseudoplasticity of the polymeric materials at molten state. It is noteworthy to mention here that the important aspect of the shear thinning behavior of neat TPU and TPU/CNF nanocomposites is mainly attributed to the higher degree of nanofiber–nanofiber and nanofiber–matrix interfacial bonding interaction that require higher magnitude of shear stress and longer dynamic relaxation time for CNF reinforced systems to flow along the flow direction.[8] The magnitude of viscosity significantly increases with the increase in nanofiber loading throughout the scanned frequency range because in case of the filled polymer matrix, the presence of homogeneously dispersed nanofibers greatly disturb the normal flow of polymer in molten state and also impose restriction on the free mobility of the polymer molecular chain segments in the flow condition. It is concluded that the TPU/CNF nanocomposites based on 15 wt % CNF content shows substantial increase in viscosity may be due to considerable restriction on flow properties that is the percolation threshold behavior of complex viscosity. The rate of increase in viscosity at low frequency region is more pronounced than that of the high frequency region, which is attributed to the nanofiber–TPU interaction and nanofiber–nanofiber frictions. At high frequency range the viscosity value of the filled system is not changed remarkably as compared to the pristine counterpart and the resultant plot seems to converge in to a single point, which may be attributed to the suitable processing of the CNF-based nanocomposites through conventional high shear internal batch mixing process.

Electrical properties

The capacitance is a function of the permittivity or dielectric constant that represents the inherent ability of the material to store electric potential energy on either surface of the sample under the influence of an alternating electric field or during a cyclic electric excitation. The energy stored is usually in the form of a nonuniform dipole distribution or ionic charge layers. The variation of dielectric constant (ε′) of the TPU/CNF nanocomposites for different wt % of CNF loading as a function of frequency in the range of 10^1–10^6 Hz at room temperature is shown in Figure 9(a). At low frequency region the dielectric constant of the TPU/CNF nanocomposites did not change up to 4 wt % CNF loading, but around 10-fold rise in dielectric constant is observed above 4 wt % CNF concentration. Furthermore, at 15 wt % CNF loading it is enhanced above 10^6 times than that of the pristine counterpart. The incorporation of nanofibers to the TPU matrix increases the dielectric constant due to its higher polarization efficiency as compared with the neat TPU. It is also linked to the possibility of the presence of an interfacial

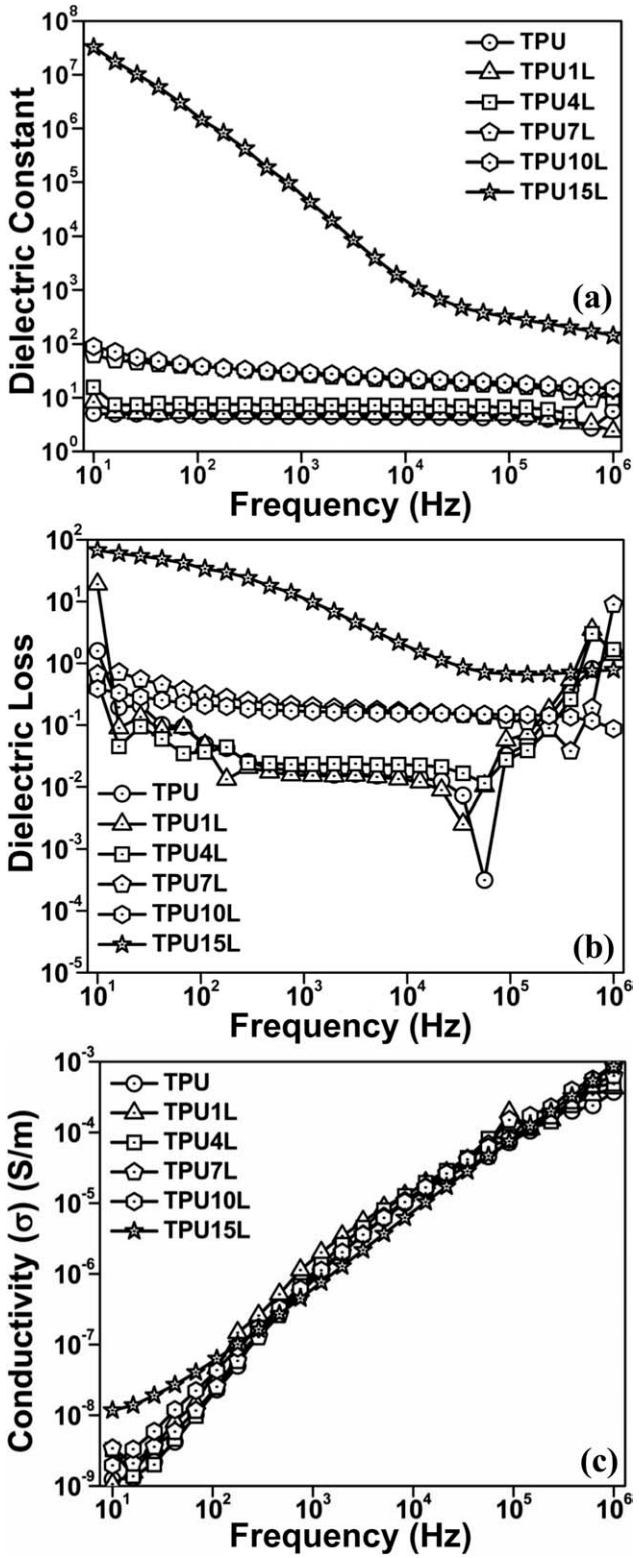

Figure 9 Variation of (a) dielectric constant, (b) loss factor (tan δ), and (c) electrical conductivity of neat TPU and TPU/CNF nanocomposites with 1, 4, 7, 10, and 15 wt % CNF loading as a function of frequency.

polarization in heterogeneous polymeric systems, which is termed as Maxwell–Wagner–Sillars effect under external electric field caused by space charge build-up, which occurs at the macroscopic interfaces, difference in conductivity and permittivity of the constituents, and microscopic field distortion.[24] The superior value of dielectric constant at relatively lower frequency region is considered to be attributed to the anomalous diffusion/polarization of the space charges present within bulk materials, microstructural internal defects associated with the polymer matrix, and electrode effects.[25] The degree of nanofiller aggregation and filler–filler crosslinking network structure is well developed at higher nanofiber loading, which further supports the polarization phenomenon between conductive clusters as a result pronounced increase in the dielectric constant is noticed at 15 wt % CNF loading.[15,26] The variation of the dielectric constant with frequency is marginal up to 10 wt % CNF content whereas, at 15 wt % CNF loading the dielectric constant decreases more rapidly with increasing frequency but the magnitude of dielectric constant is always high throughout the scanned frequency range. There is substantial reduction in dielectric constant with increased frequency because at higher frequency region, the dielectric relaxation time of the TPU matrix is substantially reduced and the interfacial polarization of the TPU/CNF nanocomposites is not sufficient enough for the internal dipoles to orient/align along the direction of the applied electric field.[27] The dielectric constant decreases exponentially with increase in frequency, which is mainly attributed to the ineffective match of interfacial polarization of TPU/CNF nanocomposites to applied external electric field at higher frequency region.[28] The polarizations lag behind the charges of the electric field at low frequency region as a result the dissipation of the electrical energy become minimum that produces higher value of dielectric constant. At high frequency range the fast alternation of direction of the electric field significantly contributes to enhance the polarization effects in the polymer matrix as a consequence the dielectric loss is minimized that prominently reduces the magnitude of dielectric constant.[29]

The variation of dissipation factor (DF) or loss tangent (tan δ) of neat TPU and the TPU/CNF nanocomposites as a function of the applied frequency at different amount of the CNF content are shown in Figure 9(b). The increase in DF with increasing CNF loading is due to the role of interfacial polarization mechanism of the heterogeneous polymeric systems. The value of loss tangent is substantially high at low frequency than that of higher frequency, which is attributed to the dipole polarization effect exhibited by the charge carriers. The dipole polarization effect tends to be minimized with further increase in frequency that results in a very small value of DF. The neat TPU and TPU/CNF nanocomposites exhibits an initial gradual decrease in tan δ with increase in

frequency followed by a plateau region to certain frequency and finally increases significantly. The high frequency range where the loss factor starts to increase is shifted towards higher frequency side with increase in CNF loading up to 7 wt % but after which it is beyond the scanned frequency range. The decrease in tan δ with the increase in frequency that is observed for both unfilled and filled TPU because the charges induced through the supply of alternating current gradually diminishes to reorient along the reversing electric field that result in a reduction in electronic oscillations.[29] The value of tan δ is very low and remains more or less frequency independent up to 10 wt % CNF concentration. Furthermore, the significantly large dissipation factor (tan δ) is observed especially for the 15 wt % CNF-filled TPU nanocomposites that showed heavy dependency on the frequency confirms an insulator to conductor electronic transition.

Figure 9(c) shows the variation of electrical conductivity as a function of experimental frequency with increasing nanofiller loading in CNF reinforced TPU nanocomposites. The conductivity of the TPU/CNF nanocomposites increases linearly with the increase of frequency as well as with weight fraction of nanofiber loading. It is assumed that an electrical conducting path and network is formed in the nanocomposites with increasing concentration of nanofibers. The change in conductivity of polymer system with frequency provides sufficient information about the overall connectivity of the conducting networks. The conductivity of the 15 wt % filled TPU nanocomposites above 100 Hz frequency is not high as compared with the pristine counterpart due to the high dielectric constant value.

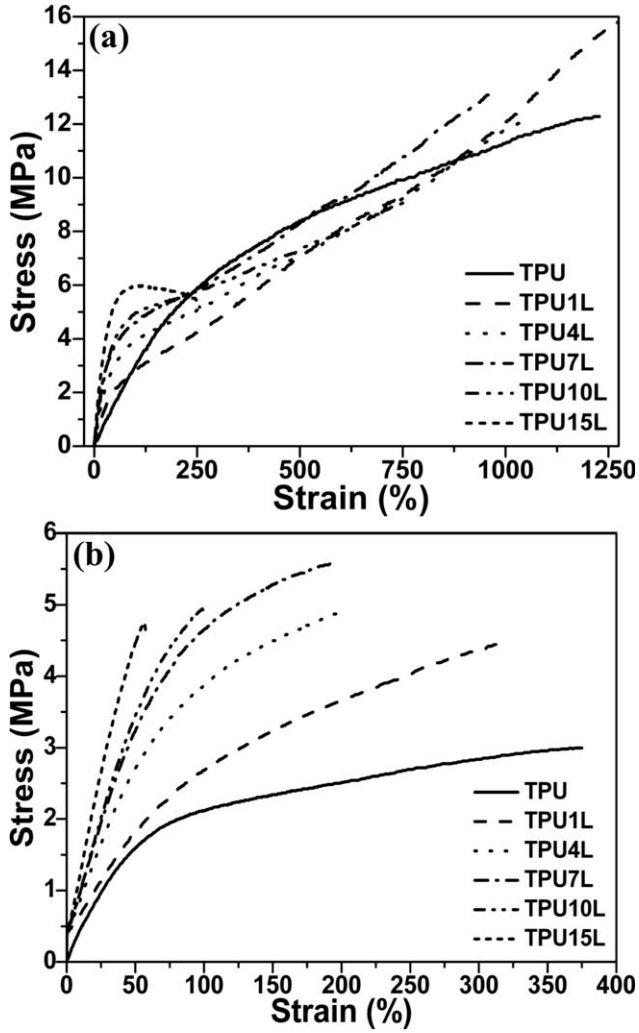

Figure 10 Typical stress–strain curve for (a) tensile and (b) tear test of neat TPU and TPU/CNF nanocomposites with 1, 4, 7, 10, and 15 wt % CNF loading.

Mechanical properties

The tensile stress–strain curves of the virgin TPU matrix and the TPU nanocomposites containing 1, 4, 7, 10, and 15 wt % CNF loading are shown in Figure 10(a). The details of the tensile data are represented in Table III. The incorporation of the nanofibers into the TPU matrix increases both the tensile strength and modulus, which indicate that the amount of nanofibers incorporated exhibits a strong reinforcing and toughing effect on the polymeric matrix. The reinforcement and hardening efficiency of the nanofibers in TPU matrix is proportional to its intrinsic mechanical properties, length to diameter ratio, weight fraction and also on the crosslinking behavior and nanofiber–matrix interfacial strength. The presence of polar functional groups on the surface of CNF implies that the strong interfacial adhesion between CNF and TPU is solely responsible for significant improvement in tensile properties. The tensile strength of the TPU/CNF nanocomposites increases first up to 7 wt % CNF concentration with respect to the TPU matrix after which it decreases as the nanofiber concentration increases above 10 wt %, because the homogeneous dispersion of nanofibers in TPU matrix is significantly affected due to highly crosslinked network structure and aggregation tendency of CNF at higher concentrations. The TPU/CNF nanocomposites show highly increased initial modulus (stiffness) at higher wt % of nanofibers, but tensile strength and elongation at break get reduced drastically, possibly due to highly crosslinking intensities of nanofiber bundles. The TPU nanocomposites with 1 wt % CNF exhibits an improvement of about 63 and 57% in the tensile strength and modulus as compare to the pure TPU.

The elongation at break of the TPU nanocomposites containing 1 wt % nanofiber loading increases by 3.82%, which is attributed to interfacial viscoelastic matrix deformation and a different failure mechanism. However, the elongation at break for

TABLE III
Tensile and Tear Test Data of TPU and TPU/CNF Nanocomposites

Sample code	Tensile strength (MPa)	Modulus, 300% elongation (MPa)	Elongation at break (%)	Tear strength (N/mm)	Hardness (shore A)
TPU	9.74	2.750	1228	40.56	72
TPU1L	15.83	2.830	1275	56.06	76
TPU4L	12.02	3.905	1053	61.57	81
TPU7L	13.08	4.610	958	69.63	84
TPU10L	9.018	4.974	760	61.76	86
TPU15L	5.990	5.900	256	63.53	89

above 1 wt % filled TPU/CNF nanocomposites decrease gradually with increase in filler loading and finally brittle failure is observed at 15 wt % CNF loading suggesting that the deformation phenomenon is associated with both interfacial deformation and degree of dispersion of CNFs in TPU matrix.[30] The mobilization of the amorphous phase of the matrix is significantly restricted by the spatial orientation of nanofibers, which prevents the dynamic deformation of matrix as a result the stiffness of TPU increases substantially.[31]

Figure 10(b) represents typical tear test stress–strain diagrams of the neat TPU and its nanocomposites. Table III shows that the tear strength of the TPU/CNF nanocomposites substantially increases at first up to 10 wt % CNF loading and then decreases at 15 wt % CNF content but still the tear strength is higher than that of neat TPU. The tear strength of nanocomposites increases significantly with increase in amounts of nanofibers because of the reinforcing effect exhibited by the uniformly dispersed CNFs. The decrease in tear strength at higher nanofiber loading is due to the aggregation tendency of the CNFs.

From Table III it is clearly seen that the hardness of the nanocomposites sheet increases continuously with increase in VGCNF content. It is concluded that the indentation hardness linearly improves because the CNFs are dispersed uniformly in the polymer and also there is good interfacial adhesive bonding between the molecular chains and the CNFs. However, the hardness of the nanocomposites above 10 wt% CNF loading does not degrade, rather it upgrade linearly even if its value is higher than that of the neat TPU matrix counterpart. It is observed that the presence of CNF clusters at higher nanofiber loading is small in size and the average distance between the aggregates is small enough as compared with the tip cross sectional area of the indentor/penetrator.[32]

CONCLUSIONS

The TPU/CNF nanocomposites have been prepared by a simple melt intercalation technique followed by compression molding. The pristine VGCNFs were treated with a mixture of concentrated sulfuric acid and nitric acid to improve their compatibility with the TPU matrix before nanocomposite preparation. The significant improvement in thermal, mechanical, rheological, and electrical properties were observed for the TPU/CNF nanocomposites by the addition of CNF. The FTIR study revealed that there exists a strong chemical interaction through hydrogen bonding among the functionalized CNFs and TPU matrix. FESEM images showed that the CNFs are uniformly dispersed within the TPU matrix at low nanofiber loading because of the strong interfacial adhesion between the VGCNFs and the TPU matrix, whereas small clusters are visualized at high CNF content. It was concluded from HRTEM pictures that the CNFs are homogeneously dispersed in the form of individual nanofibers and network was developed at high nanofiber loading. POM and AFM microphotographs showed that the CNFs were effectively dispersed via either covalent or ionic bond formation between CNF and TPU. TGA experiment revealed that the addition of nanofiber improved the thermal degradation stability. The T_g and crystallization melting temperature of the soft segments of TPU matrix was not changed greatly by the inclusion of CNF. The DMTA test showed that The T_g was greatly enhanced because of the selective chemical linkage of the CNFs with the TPU molecular chains. The storage modulus of the nanocomposites both below and above the T_g showed a higher value as compared to the control compound, which was attributed to the high aspect ratio of CNFs that effectively exhibit reinforcing effect and load transfer mechanism from continuous phase to dispersed phase. The rheological measurement depicted that the melt viscosity and shear modulus are increased by the inclusion of CNFs. The practice of sufficient shear thinning behavior of the nanocomposites is legible from processing point of view. The electrical test showed that the dielectric constant and dissipation factor is more significant for TPU/CNF nanocomposites and the conductivity was enhanced by the applied frequency. The results of mechanical property tests indicated that the tensile strength, tear strength, and hardness of the nanocomposites were

significantly improved with the incorporation of CNFs. The material properties of the TPU/CNF nanocomposites were improved satisfactorily so that the nanocomposites may be suitable for potential product applications in desired field.

References

1. Al-Saleh, M. H.; Sundararaj, U. Carbon 2009, 47, 2.
2. Gunes, I. S.; Cao, F.; Jana, S. C. J Polym Sci B: Polym Phys 2008, 46, 1437.
3. Gunes, I. S.; Jimenez, G. A.; Jana, S. C. Carbon 2009, 47, 981.
4. Jimenez, G. A.; Jana, S. C. Carbon 2007, 45, 2079.
5. Jimenez, G. A.; Jana, S. C. Polym Eng Sci 2009, 49, 2020.
6. Powers, D. S.; Vaia, R. A.; Koerner, H.; Serres, J.; Mirau, P. A. Macromolecules 2008, 41, 4290.
7. Barick, A. K.; Tripathy, D. K. Compos A: Appl Sci Manufact 2010, 41, 1471.
8. Lozano, K.; Bonilla-Rios, J.; Barrera, E. V. J Appl Polym Sci 2001, 80, 1162.
9. Jiang, F.; Hu, G.; Wu, S;Wei, Y.; Zhang, L. Polym Polym Compos 2008, 16, 471.
10. Sui, G.; Zhong, W. H.; Ren, X.; Wang, X. Q.; Yang, X. P. Mater Chem Phys 2009, 115, 404.
11. Chatterjee, A.; Deopura, B. L. J Appl Polym Sci 2008, 100, 3574.
12. Sui, G.; Zhong, W. H.; Fuqua, M. A.; Ulven, C. A. Macromol Chem Phys 2207, 208, 1928.
13. Barick, A. K.; Tripathy, D. K. Mater Sci Eng A Struct Mater: Prop Microstruct Process 2010, 527, 812.
14. Gunes, I. S.; Cao, F.; Jana, S. C. Polymer 2008, 49, 2223.
15. Liang, G. D.; Tjong, S. C. IEEE Trans Dielect Elect Insul 2008, 15, 214.
16. Eitan, A.; Fisher, F. T.; Andrews, R.; Brinson, L. C.; Schadler, L. S. Compos Sci Technol 2006, 66, 1162.
17. Kumar, S.; Rath, T.; Mahaling, R. N.; Reddy, C. S.; Das, C. K.; Pandey, K. N.; Srivastava, R. B.; Yadaw, S. B. Mater Sci Eng: B Adv Funct Solid-State Mater 2007, 141, 61.
18. Menard, K. P. Dynamic Mechanical Analysis: A Practical Introduction; CRC Press LLC: Florida, 1999.
19. Yang, S.; Taha-Tijerina, J.; Serrato-Diaz, V.; Hernandez, K.; Lozano, K. Compos B: Eng 2007, 38, 228.
20. Krishnamoorti, R.; Vaia, R. A.; Giannelis, E. P. Chem Mater 1996, 8, 1728.
21. Krishnamoorti, R.; Giannelis, E. P. Macromolecules 1997, 30, 4097.
22. Mitchell, C. A.; Bahr, J. L.; Arepalli, S.; Tour, J. M.; Krishnamoorti, R. Macromolecules 2002, 35, 8825.
23. Lozano, K.; Yang, S.; Zeng, Q. J Appl Polym Sci 2004, 93, 155.
24. Tsangaris, G. M.; Psarras, G. C.; Kouloumbi, N. J Mater Sci 1998, 33, 2027.
25. Borah, J.; Mahapatra, S. S.; Saikia, D.; Karak, N. Polym Degrad Stab 2006, 91, 2911.
26. Goyal, R. K.; Jagadale, P. A.; Mulik, U. P. J Appl Polym Sci 2009, 111, 2071.
27. Sui, G.; Zhong, W. H.; Fuqua, M. A.; Ulven, C. A. Acta Mater 2008, 56, 2381.
28. Li, Y. C.; Li, R. K. Y.; Tjong, S. C. J Nanomater 2010, 261748, 1.
29. Panwar, V.; Sachdev, V. K.; Mehra, R. M. Eur Polym J 2007, 43, 573.
30. Shi, Y.; Feng, X.; Wang, H.; Lu, X.; Shen, J. J Appl Polym Sci 2007, 104, 2430.
31. Vidhate, S.; Shaito, A.; Chung, J.; D'Souza, N. A. J Appl Polym Sci 2009, 112, 254.
32. Galetz, M. C.; Blaβ, T.; Ruckdäschel, H.; Sandler, J. K. W.; Altstädt, V.; Glatzel, U. J Appl Polym Sci 2009, 104, 4173.